Structural control and magnetic properties of electrodeposited Co nanowires

Xue Wei Wang, Guang Tao Fei*, Peng Tong, Xi Jin Xu, Li De Zhang

Key Laboratory of Materials Physics, Institute of Solid State Physics, Hefei Institutes of Physical Science, Chinese Academy of Sciences, P.O. Box 1129, Hefei 230031, PR China

Abstract

Co nanowires with a preferred orientation were fabricated by direct current electrodeposition into the pores of porous anodic alumina membrane, and the structure of Co nanowires was studied by X-ray diffraction and high-resolution transmission electron microscopy with selected-area electron diffraction. It is found that the crystal structure of Co nanowires lies on the deposition potential. When electrodeposition is performed far from equilibrium conditions, i.e., at a high potential, face-centered cubic Co nanowires are deposited, while hexagonal close packing Co nanowires are formed at the low potential. The experimental results indicate that the orientation of the nanowires has effects on the coercivity for both hexagonal close packing (hcp) and face-centered cubic (fcc) Co.
© 2007 Elsevier B.V. All rights reserved.

PACS: 51.60.+a; 82.45.Aa

Keywords: A1. Nanostructures; A2. Electrochemical growth; B1. Metals; B2. Magnetic materials

1. Introduction

Magnetic nanowires have attracted much interest in recent years for their potential applications in high-density magnetic recording devices [1,2]. To realize these applications, the structure and the growth direction of nanowires need to be controlled precisely because the magnetic properties are related to these. The synthesis and control of the magnetic nanostructure on a large scale is a challenging issue in the field of material science. One of the solutions is the method to combine electrodeposition with template. Electrodeposition method has several advantages over dry processes [3], for example, the deposition parameters can be easily adjusted. These parameters, such as pH value, deposition potential and temperature, are responsible for the control of the structure. Several researchers have reported that the pH value of the bath solution significantly affects the structure of Co film formed by electrodeposition. A solution with a low pH value (<2.5) was reported to favor face-centered cubic (fcc) Co film [4–6], whereas a high pH value (>2.5) or a high temperature system favored the formation of hexagonal close packing (hcp) Co film [7]. For Co nanowires, several reports said that the acidity or pH value of electrolyte has effects on the structure of Co nanowires [8–11]. That is to say, the hcp and fcc Co nanowires can be obtained by adjusting pH value of electrolyte. However, Co nanowires with the fcc structure prepared by adjusting pH value were polycrystalline [9]. It is of interest to fabricate Co nanowire arrays with a preferred orientation and to investigate their magnetic properties, because the nanowires with a preferred orientation exhibit excellent magnetic properties, such as large anisotropy, large coercivity, high remanence, and so on [12].

Co nanowires have been electrodeposited into the pores of porous anodic alumina membrane (PAAM) [1,9–11] and polycarbonate [13–16]. Nevertheless, the PAAM template is commonly used because of its excellent properties, such

---

*Corresponding author. Fax: +86 551 5591434.

E-mail address: gtfei@issp.ac.cn (G.T. Fei).

as corrosion resistance and decorative properties, and nanopore regularity. Highly ordered Co nanowire arrays with uniform diameter are essential for studying their properties and application in the high-density magnetic recording devices in future. So, in this work, we fabricated Co nanowire arrays with a preferred orientation in the pores of the PAAM, and obtained the different structures (fcc and hcp) by adjusting the deposition potential. The magnetic properties of the fcc and hcp Co nanowires have also been investigated.

2. Experiment

The PAAM templates were prepared by a two-step anodization process as described previously [17,18]. We have modified the procedure to improve the nanopore regularity of the PAAM template [19]. To be brief, prior to anodizing, high-purity aluminum foils (99.999%) were annealed in a vacuum of 10^{-3} Pa at 500 °C for 5 h to remove the mechanical stress and obtain homogenous structure. The two steps of anodization were performed in 0.3 M oxalic acid under 40 V and 5 °C. After the second anodization, the remaining aluminum was etched by saturated $SnCl_4$ solution. The alumina barrier layer was then dissolved in 5 wt% H_3PO_4 solution at 30 °C. Finally, a layer of Au film (about 200 nm in thickness) was sputtered onto one side of the PAAM template to serve as the working electrode in a two-electrode plating cell. The electrolyte used in this work contained 200 g/L Co-$SO_4 \cdot 7H_2O$ and 40 g/L H_3BO_3. According to the previous reports [9–11], the pH value of solution was adjusted to 5.5 with 1 M H_2SO_4. Direct current (DC) electrodeposition was performed at the potentials of −1.45 and −3 V, which are the potentials between graphite anode and Au film cathode on the PAAM in a common two-electrode plating cell, at room temperature.

The phase structures of Co nanowire arrays were characterized by X-ray diffraction (XRD, Philips X'Pert) with Cu Kα_1 radiation ($\lambda = 0.154056$ nm). The morphologies of Co nanowire arrays were observed with field-emission scanning electron microscopy (FE-SEM, FEI, Sirion 200), and the morphology of the single Co nanowire was characterized with high-resolution transmission electron microscopy (HRTEM, JEOL-2010) with selected-area electron diffraction (SAED). A Physical Property Measurement System (PPMS, Quantum Design) was used to measure the magnetic properties of the samples at room temperature.

3. Results and discussion

The morphologies of Co nanowire arrays are shown in Fig. 1. It can be seen from Fig. 1(a) that a large number of Co nanowires were liberated from the PAAM template and bundled together after partly dissolving the PAAM. Fig. 1(b) is the cross-sectional SEM image of Co nanowire arrays. As shown in Fig. 1(b), Co nanowires have the
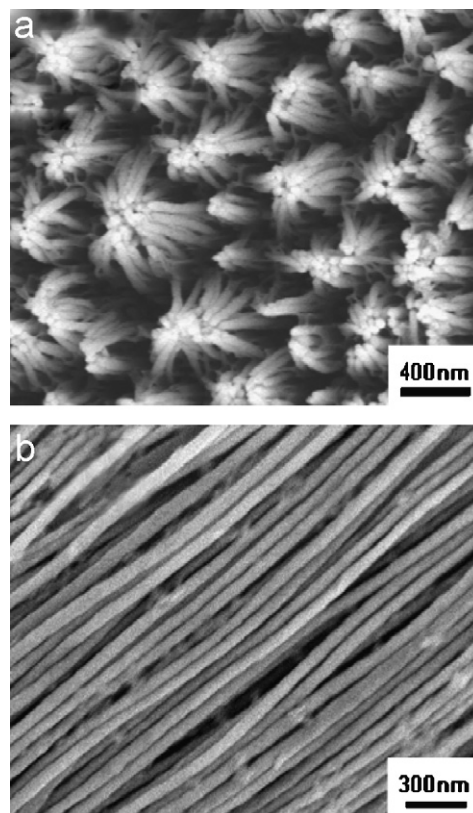

Fig. 1. FE-SEM images of Co nanowires after partly etching the PAAM: (a) top view and (b) cross-sectional view.
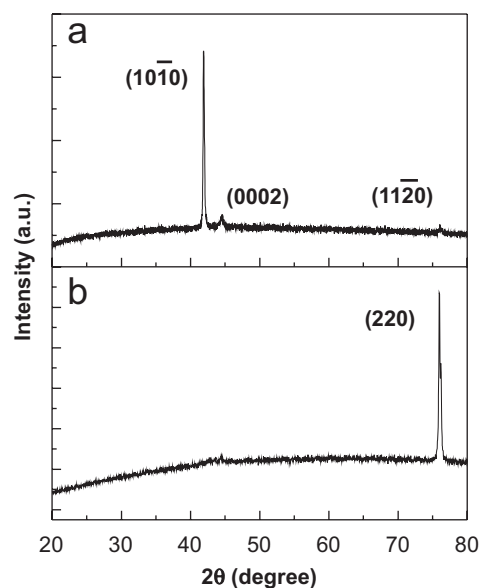

Fig. 2. XRD patterns of Co nanowire arrays prepared under the different conditions: (a) the potential of −1.45 V and (b) the potential of −3 V.

uniform diameter because of the finite effects of the pores of the PAAM.

In Fig. 2 are shown the XRD patterns of as-prepared Co nanowire arrays. Fig. 2(a) shows the typical XRD pattern of the sample fabricated under the condition of the potential of −1.45 V. It can be seen that all peaks can be
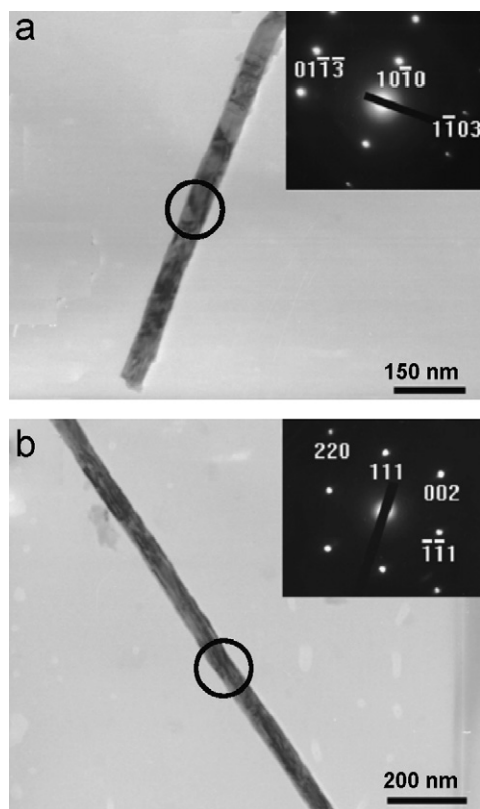
Fig. 3. TEM images and SAED of Co nanowires: (a) hcp structure and (b) fcc structure.

Fig. 4. HRTEM image and corresponding SAED of Co nanowire with fcc structure.

indexed to the hcp phase, and match well with the standard diffraction peaks of Co (JCPDF 89-4308). The intensity for $(1\,0\,\bar{1}\,0)$ planes is very strong and higher than others, which indicates that the c-axis is perpendicular to the axis direction of nanowires. The XRD pattern for the sample fabricated under the condition of the potential of $-3\,V$ is shown in Fig. 2(b). A predominant XRD peak at $2\theta = 75.8°$ has been observed in Fig. 2(b). It is well known that the standard diffraction of hcp Co (JCPDF 89-4308) and fcc Co (JCPDF 89-4307) both have the peaks at $2\theta = 44.2°$, $75.8°$. So, it is difficult to judge the structure of the sample fabricated at the potential of $-3\,V$ from the XRD pattern shown in Fig. 2(b) for there is only one peak appearing.

TEM image and SAED are performed to further confirm the structure of the samples fabricated under the different conditions. Fig. 3(a) shows a typical TEM image of a single Co nanowire fabricated at the potential of $-1.45\,V$. It can be seen from Fig. 3(a) that the diffraction pattern which is corresponding to the area signed by the circle can be indexed to hcp structure, and Co nanowire has a preferred orientation along the $[1\,0\,\bar{1}\,0]$ direction. This is in accord with the result of XRD shown in Fig. 2(a). In Fig. 3(b) is shown a typical image of a single Co nanowire fabricated at the potential of $-3\,V$. According to SAED which corresponds to the area signed by the circle in the inset of Fig. 3(b), it is found that the structure of the nanowire is fcc. Meanwhile, the preferred orientation of the nanowire is
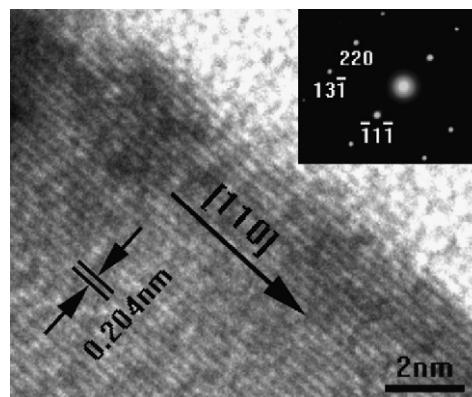
along the $[1\,1\,0]$ direction. HRTEM was used to further prove the fcc structure of Co nanowires (Fig. 4). It can be seen from the lattice fringe and the corresponding SAED in Fig. 4 that Co nanowire fabricated at the potential of $-3\,V$ has the fcc structure.

Hcp structure is universal for electrodeposited Co. It is well known that Co with fcc structure, which is stable at temperatures above $422\,°C$, can be obtained from electrodeposition at lower pH value [9]. Our experiments show that the DC electrodeposition process at the low potential ($-1.45\,V$), i.e., small current density would result in the hcp structure of Co nanowires (see Figs. 2(a) and 3(a)). However, the fcc structure of Co nanowires has been obtained at the potential of $-3\,V$ (see Figs. 2(b) and 3(b)). In this condition, the process of electrodeposition is far from the equilibrium because the current density is big at the high potential. Meanwhile, at the high potential, the adsorption of hydrogen from the acidic solution on the electrode surface will happen, and will induce a thermodynamic to kinetic transition during the electrodeposition [20]. It has been reported that the fcc structure of electrodeposited Co film was formed at a high potential [21]. Nakahara and Mahajan [6] suggested a mechanism for the formation of Co with fcc structure at low pH value. According to their opinions, the formation of fcc Co, which is actually metastable Co hydride (fcc), is promoted by the electrodeposition of atomic hydrogen. We think that the mechanism proposed by Nakahara and Mahajan can also be applied to the formation of Co nanowires with fcc structure in our case. The formation of a metastable Co hydride (fcc) is possible at the high potential because the evolution of hydrogen is greatly increased with an increasing potential. Therefore, at the high deposition potential, the fcc structure of Co nanowires can be formed.

At the high potential, Co nanowires with fcc structure have a preferred orientation along the $[1\,1\,0]$ direction. As is well known, the growth of nanowires is a result of a competitive mechanism after the nucleation. It was reported that the competition between the adsorption and desorption of hydrogen ions exists along with the growth of metallic nanowires [22]. For the deposition of Co

nanowires with fcc structure, the adsorption of hydrogen ions on the cathode stabilizes the (1 1 0) face [23]. In our case, the high deposition potential may make much hydrogen ions accumulate on the cathode, so the growth of (2 2 0) plane is favorable with the aid of the hydrogen ions adsorption for Co nanowires with fcc structure. Therefore, Co nanowires have not only the fcc structure but also a preferred orientation along the [1 1 0] direction.

The magnetic properties of Co nanowire arrays embedded in the PAAM are closely related to the structure. The magnetic hysteresis loops were measured at room temperature for Co nanowire arrays with hcp and fcc structures, where the applied field is parallel and perpendicular to the nanowire's axis (Fig. 5). It is worth mentioning that bigger coercivity and squareness will occur when the applied field is parallel to the nanowire's axis for Co nanowire arrays with both hcp and fcc structures (Fig. 5). However, the coercivity and squareness of fcc Co nanowire arrays are larger than those of hcp Co nanowire arrays when the applied field is parallel to the nanowire's axis.

It is well known that ferromagnetic material has an easy magnetization direction. In the case of hcp Co, the easy magnetization direction is along the c-axis [24]. In our experiments, the c-axis is perpendicular to the axis direction of Co nanowires with hcp structure. When the applied field is parallel to the nanowire's axis, hcp Co

nanowire arrays have a coercivity of 520 Oe in our experiments. This result is almost the same as the reported values of the coercivity for hcp Co nanowires with the c-axis perpendicular to the nanowire's axis [8,10,25], and lower than the reported values of the coercivity for hcp Co nanowires with the c-axis parallel to the nanowire's axis [10,26,27]. Some works [8,9,27] have reported that the effective anisotropy of the magnetic nanowire arrays comes from the competition between the magnetocrystalline anisotropy and the shape anisotropy. Magnetocrystalline anisotropy of the hcp Co nanowires will make the magnetic moment arrange along the c-axis, i.e. perpendicular to the nanowire's axis in our experiments, but the shape anisotropy tends to arrange the magnetic moment along the axis of the nanowires [9]. So, the competition between magnetocrystalline anisotropy and shape anisotropy results in a relatively weak effective anisotropy along the nanowire's axis, which leads to the low coercivity [9]. Comparing the reported results [10,26,27] with our value, we can see that the orientation of the hcp Co nanowires has effects on the coercivity. For the fcc Co nanowires with the orientation along the [1 1 0] direction, the coercivity is about 1260 Oe in our experiments, which is lower than the result of fcc Co nanowires with the orientation along the [1 1 1] direction obtained by Li et al. [9]. This further indicates that the orientation of Co nanowires has effects on the coercivity.

4. Conclusions

In summary, we have fabricated Co nanowire arrays with hcp and fcc structures by adjusting the potential during the DC electrodeposition. At the potential of −1.45 V, Co nanowire arrays with hcp structure were formed, while Co nanowire arrays with fcc structure were obtained at the potential of −3 V. The results of magnetic measurements show that the orientation of the nanowires has effects on the coercivity for both hcp and fcc Co.
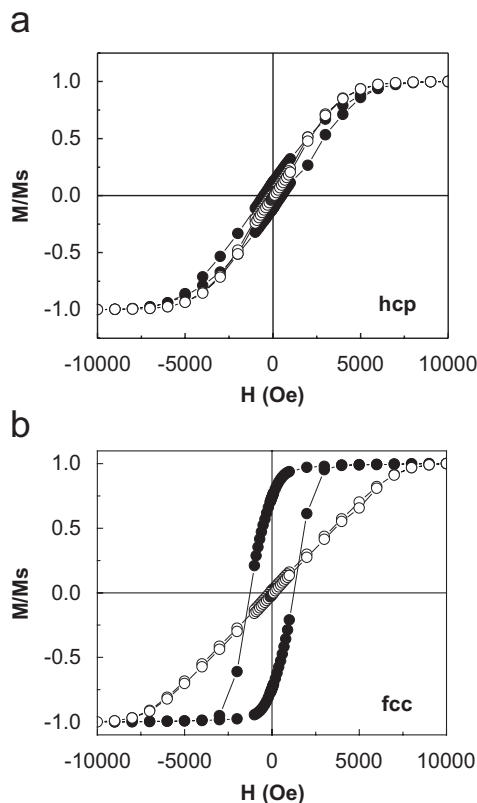
Acknowledgments

Fig. 5. Magnetic hysteresis loops of Co nanowire array embedded in the PAAM: (a) hcp structure and (b) fcc structure. (—●—) Denotes field applied parallel to nanowire's axis and (—○—) denotes field applied perpendicular to nanowire's axis.

References

[1] K. Nielsch, R.B. Wehrspohn, J. Barthel, J. Kirschner, U. Gosele, S.F. Ficher, H. Kronmuller, Appl. Phys. Lett. 79 (2001) 1360.
[2] C. Ross, R. Chantrell, M. Hwang, M. Farhoud, T. Saves, Y. Hao, H. Smith, F. Ross, M. Redidal, F. Himphrey, Phys. Rev. B 62 (2000) 14252.
[3] J. Yahalom, O. Zadok, J. Mater. Sci. 21 (1987) 499.
[4] J.W. Dini, Electrodeposition, Noyes, Park Ridge, NJ, 1993, p. 156.

[5] M.H. Gelchinski, L. Gal-Or, J. Yahalom, J. Electrochem. Soc. 129 (1982) 2433.

[6] S. Nakahara, S. Mahajan, J. Electrochem. Soc. 127 (1980) 283.

[7] K.I. Gaigalas, A.I. Bodenevas, Y.Y. Matulis, Trudy Akad, Nank Lit. SSR B 4 (1968) 59.

[8] A. Encinas, M. Demand, J.-M. George, L. Piraux, IEEE Trans. Magn. 38 (2002) 2574.

[9] F. Li, T. Wang, L. Ren, J. Sun, J. Phys.: Condens. Matter 16 (2004) 8053.

[10] M. Darques, A. Encinas, L. Vila, L. Piraux, J. Phys. D 37 (2004) 1411.

[11] M. Darques, L. Piraux, A. Encinas, P. Bayle-Guillemaud, A. Popa, U. Ebels, Appl. Phys. Lett. 86 (2005) 072508.

[12] H. Pan, B.H. Liu, J.B. Yi, C. Poh, S.H. Lim, J. Ding, Y.P. Feng, C.H.A. Huan, J.Y. Lin, J. Phys. Chem. B 109 (2005) 3094.

[13] Y. Henry, K. Ounadjela, L. Piraux, S. Dubois, J.-M. George, J.-L. Duvail, Eur. Phys. J. B 20 (2001) 35.

[14] V. Scarani, B. Doudin, J.-P. Ansermet, J. Magn. Magn. Mater. 205 (1999) 241.

[15] A. Kazadi Mukenga Bantu, J. Rivas, G. Zaragoza, M.A. Lopez-quineta, M.C. Blanco, J. Appl. Phys. 89 (2001) 3393.

[16] M.L. Tian, J.G. Wang, J. Kurtz, T.E. Mallouk, M.H.W. Chan, Nano Lett. 3 (2003) 919.

[17] H. Masuda, K. Fukuda, Science 268 (1995) 1466.

[18] A.P. Li, F. Müller, A. Birner, K. Nielsch, U. Gösele, J. Vas. Sci. Technol. A 17 (1999) 1428.

[19] X.W. Wang, G.T. Fei, X.J. Xu, Z. Jin, L.D. Zhang, J. Phys. Chem. B 109 (2005) 24326.

[20] J.A. Switzer, H.M. Kothari, E.W. Bohannan, J. Phys. Chem. B 106 (2002) 4027.

[21] T. Cohen-Hyams, W.D. Kaplan, J. Yahalom, Electrochem. Solid-State Lett. 5 (2002) C75.

[22] H. Pan, H. Sun, C. Poh, Y. Feng, J. Lin, Nanotechnology 16 (2005) 1559.

[23] E. Budevski, G. Staikov, W.J. Lorenz, Electrochemical Phase Formation and Growth: An Introduction to the Initial Stage of Metal Deposition, VCH, New York, 1996, p. 267.

[24] C. Kittel, Introduction to Solid State Physics, Wiley, New York, 1976, p. 487.

[25] H.N. Hu, H.Y. Chen, S.Y. Yu, J.L. Chen, G.H. Wu, F.B. Meng, J.P. Qu, Y.X. Li, H. Zhu, J.Q. Xiao, J. Magn. Magn. Mater. 295 (2005) 257.

[26] A. Ursache, J.Y. Goldbach, T.P. Russell, M.T. Tuominen, J. Appl. Phys. 97 (2005) 10J322.

[27] K. Ounadjela, R. Ferré, L. Louail, J.M. George, J.L. Maurice, L. Piraux, S. Dubois, J. Appl. Phys. 81 (1997) 5455.